

## RESEARCH ARTICLE

# Functionally distinct roles for T and Tbx6 during mouse development

Amy K. Wehn<sup>\*</sup>, Deborah R. Farkas<sup>‡</sup>, Carly E. Sedlock<sup>§</sup>, Dibya Subedi<sup>¶</sup> and Deborah L. Chapman<sup>\*\*</sup>

## ABSTRACT

The mouse T-box transcription factors T and Tbx6 are co-expressed in the primitive streak and have unique domains of expression; T is expressed in the notochord, while Tbx6 is expressed in the presomitic mesoderm. T-box factors are related through a shared DNA binding domain, the T-domain, and can therefore bind to similar DNA sequences at least *in vitro*. We investigated the functional similarities and differences of T and Tbx6 DNA binding and transcriptional activity *in vitro* and their interaction genetically *in vivo*. We show that at one target, *Dll1*, the T-domains of T and Tbx6 have different affinities for the binding sites present in the mesoderm enhancer. We further show using *in vitro* assays that T and Tbx6 differentially affect transcription with Tbx6 activating expression tenfold higher than T, that T and Tbx6 can compete at target gene enhancers, and that this competition requires a functional DNA binding domain. Next, we addressed whether T and Tbx6 can compete *in vivo*. First, we generated embryos that express Tbx6 at greater than wild-type levels embryos and show that these embryos have short tails, resembling the *T* heterozygous phenotype. Next, using the dominant-negative *TWIs* allele, we show that *Tbx6*<sup>+/-</sup> *TWIs*<sup>+/+</sup> embryos share similarities with embryos homozygous for the *Tbx6* hypomorphic allele *rib-vertebrae*, specifically fusions of several ribs and malformation of some vertebrae. Finally, we tested whether Tbx6 can functionally replace T using a knockin approach, which resulted in severe *T* null-like phenotypes in chimeric embryos generated with ES cells heterozygous for a *Tbx6* knockin at the *T* locus. Altogether, our results of differences in affinity for DNA binding sites and transcriptional activity for T and Tbx6 provide a potential mechanism for the failure of Tbx6 to functionally replace T and possible competition phenotypes *in vivo*.

**KEY WORDS:** T, Tbx6, Brachyury, Mouse, T-box, Mesoderm

## INTRODUCTION

The T-box proteins constitute a family of transcription factors that are related through a shared DNA binding domain, the T-domain that allows family members to bind similar DNA sequences. Therefore, these related factors have the potential to regulate the

expression of the same target genes. However, T-box factors may differ in how they regulate transcription once they bind to DNA; acting as transcriptional activators, repressors or as both. Interestingly, in addition to facilitating DNA binding, the T-domain can also interact with chromatin remodelers (Beisaw et al., 2018; Istaces et al., 2019; Lewis et al., 2007; Miller et al., 2008, 2010), including histone methyltransferases, demethylases, acetyltransferases and deacetyltransferases, and these interactions regulate the permissiveness of the chromatin environment. Outside of the T-domain, the proteins share little similarity. T-box transcription factors are indispensable for normal development of organisms ranging from worms to humans. Homozygous loss of these family members can have catastrophic effects on the developing embryos often leading to lethality with phenotypes highlighting the importance of these proteins in diverse processes, including cell proliferation, migration, cell fate and tissue morphogenesis (reviewed in Papaioannou, 2014). Interestingly, heterozygosity for T-box factors can also have phenotypic consequences. For example, the founding member of this family, Brachyury or T, was initially identified by the short-tailed heterozygous phenotype (Dobrovolskaia-Zavadskaia, 1927). In humans, these heterozygous conditions can lead to syndromes, including Holt-Oram Syndrome (HOS, *TBX5*), ulna mammary syndrome (UMS, *TBX3*), DiGeorge syndrome (*TBX1*), spondylocostal dysostosis (*TBX6*) and cleft palate and ankyloglossia (*TBX22*) (reviewed in Ghosh et al., 2017). Therefore, maintaining the proper levels of these transcription factors is also critical for normal development.

In the mouse, T and Tbx6 are critical for mesoderm formation and differentiation. *T* is expressed in the notochord and primitive streak (PS) with T expression downregulated as cells leave the streak (Wilkinson et al., 1990). Likewise, *Tbx6* is expressed in the PS but is also expressed in the presomitic paraxial mesoderm (PAM) with expression being downregulated as the somites are formed (Chapman et al., 1996). As previously stated, heterozygosity for *T* results in loss of posterior structures resulting in variable (shortened) tail lengths. Homozygous loss of *T* leads to more pronounced axis truncations, with the embryonic axis terminating just caudal to the forelimb; embryonic lethality by embryonic day (e) 10.5 is due to the failure to form the extraembryonic allantois (Herrmann et al., 1990). These variable phenotypes for the *T* hetero- and homozygous null embryos suggest that different levels of T are required along the axis, with highest T levels required for more posterior development (MacMurray and Shin, 1988; Stott et al., 1993). The dosage sensitivity of the axis to T levels is not limited to mice as bobtail dogs (Haworth et al., 2001) and Manx cats (Buckingham et al., 2013) also display short tails when heterozygous for *T* mutations. Development is also sensitive to Tbx6 levels; spondylocostal dysostosis in humans can be caused by mutations in *TBX6* that reduce its transcriptional activity (Sparrow et al., 2013). We and others have further shown that the spontaneous mouse mutant *rib-vertebrae* is a *Tbx6* regulatory mutation that results in decreased

Department of Biological Sciences, University of Pittsburgh, Pittsburgh, PA 15260, USA.

<sup>\*</sup>Present address: Alliance Management, Foundation Medicine, Cambridge, MA 02141, USA. <sup>‡</sup>Present address: WISER, Educational Development, UPMC, Pittsburgh, PA 15213, USA. <sup>§</sup>Present address: Department of Internal Medicine, Jefferson University Hospitals, Philadelphia, PA 19107, USA. <sup>¶</sup>Present address: Department of Pediatrics, NYU Langone, New York, NY 10016, USA.

<sup>\*\*</sup>Author for correspondence (dlc7@pitt.edu)

 D.L.C., 0000-0002-8695-6243

This is an Open Access article distributed under the terms of the Creative Commons Attribution License (<https://creativecommons.org/licenses/by/4.0>), which permits unrestricted use, distribution and reproduction in any medium provided that the original work is properly attributed.

Received 19 July 2020; Accepted 21 July 2020

levels of *Tbx6* expression, and fusions of the ribs and vertebrae and shortening of the axis due to vertebral malformations (Watabe-Rudolph et al., 2002; White et al., 2003). Homozygous loss of *Tbx6* results in the improper patterning of ~9 anterior somites and the replacement of more posterior PAM with neural tissue (Chapman and Papaioannou, 1998). *Tbx6* is initially expressed in the *T* null, but expression is lost once the mutant phenotype becomes obvious (Chapman et al., 1996). *T* continues to be expressed in the enlarged tail bud region of the *Tbx6* mutant (Chapman and Papaioannou, 1998). This data suggests that neither *T* nor *Tbx6* can compensate for the loss of the other in these mutant situations.

We sought to examine why these related factors could not compensate for each other despite sharing a similar DNA binding domain and both functioning as transcriptional activators. We hypothesized that there were differences in their binding and activity that contributed to this failure to compensate. We first tested the binding affinities of *T* and *Tbx6* for *T* binding sites in a known target for both, *Dll1*. We then examined how each affects transcription from several enhancers, including enhancers of *in vivo* targets. These results suggest not only different binding affinities and transcriptional activity, but also that these related factors can compete with each other and that competition is dependent on the *T*-domain. Given this *in vitro* competition, we examined the effect of overexpressing *Tbx6* in its endogenous domain and the *T/Tbx6* genetic interactions using the *T<sup>Wis</sup>* dominant allele and *Tbx6* loss-of-function allele. In both situations we found evidence that suggested competition, specifically overexpression of *Tbx6* resulted in *T*-like short tail phenotypes, while *T<sup>Wis</sup>/+ Tbx6* +/- embryos share similarities with *Tbx6* hypomorphs. Finally, we tested the ability of *Tbx6* to functionally replace *T* using a knockin approach in mice. We found that *Tbx6* was not sufficient to rescue a heterozygous loss of *T*

when *Tbx6* is expressed in the *T* endogenous domain. Moreover, we found that *Tbx6* expression in the *T* domain inhibited normal development of chimeric embryos. Altogether, our results suggest that *T* and *Tbx6* differentially regulate downstream target gene expression, through either DNA binding affinities, transcriptional activity or both, that they can compete at some targets, and that this competition is mediated by the DNA binding domain.

## RESULTS

### *T* and *Tbx6* DBD have different affinities for *T*-box binding sites in the *Dll1*-*msd* enhancer

Genetic, biochemical and transcriptional assays demonstrated that *T*-box and Wnt signaling are critical for controlling *Dll1* expression in the PSM (Beckers et al., 2000b; Hofmann et al., 2004; White and Chapman, 2005; White et al., 2003). *Dll1* is a target of both *T* and *Tbx6* (Hofmann et al., 2004; White and Chapman, 2005). Beckers and colleagues identified a *Dll1* '*msd*' enhancer element capable of driving *lacZ* reporter expression in the mouse PSM (Beckers et al., 2000a). This *Dll1*-*msd* enhancer contains *T*-box and TCF/LEF binding sites that are required for enhancer activity *in vitro* and *in vivo* (Hofmann et al., 2004; White and Chapman, 2005). To further understand similarities and differences between *T* and *Tbx6* target gene regulation, we first measured the affinities of the *T* and *Tbx6* *T*-domain for these binding sites.

We previously showed using electrophoretic mobility shift assays (EMSA) that full-length *Tbx6* can bind both *T*-box binding site (BS) 1 (5'-AGGTGTTG-3') and BS2 (5'-AGGTGTGA-3') in the *Dll1*-*msd* enhancer (White and Chapman, 2005). Here we test the affinities of the DNA binding domains (DBD) of *T* and *Tbx6* for the four putative *T*-box BSs in this enhancer (Fig. 1A). Similar to the full-length *Tbx6* protein, the *Tbx6*-DBD could shift both BS1

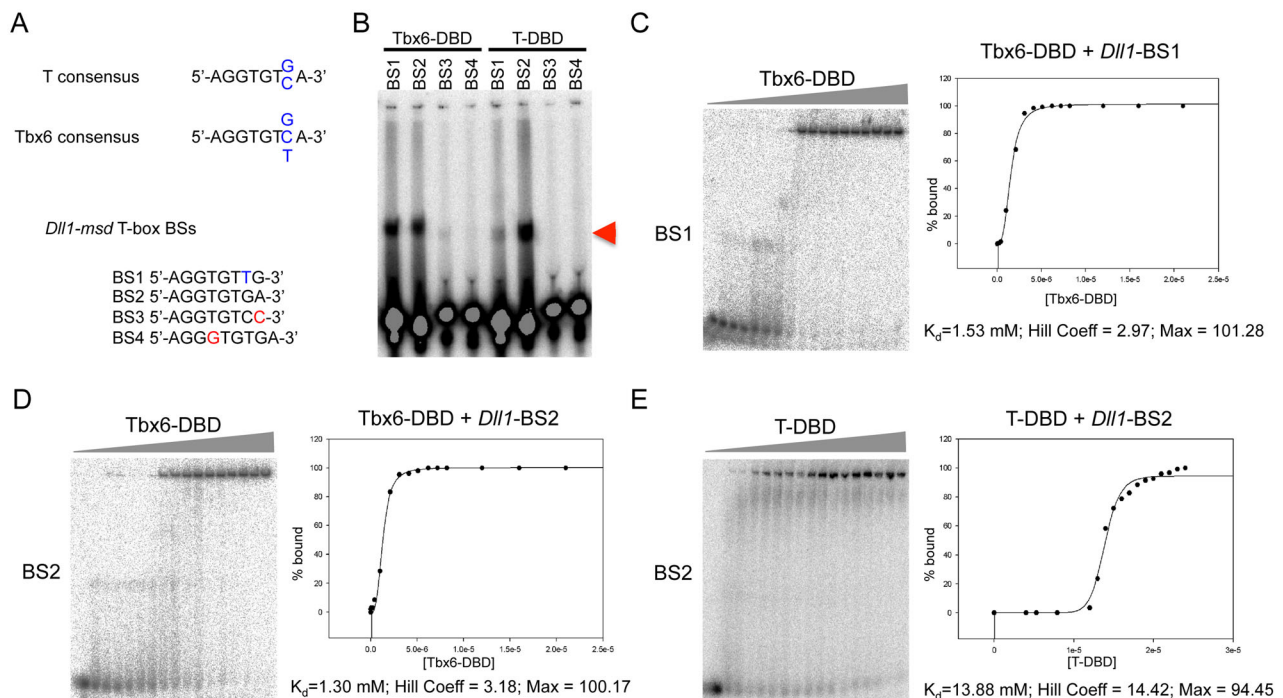


**Fig. 1. Binding of *Tbx6* and *T* DNA binding domains to the *T*-box binding sites in the *Dll1*-*msd* enhancer.** (A) EMSAs using the DBDs of *Tbx6* and *T* and the four *T*-box binding sites (BS) found in the *Dll1*-*msd* enhancer are shown with the variable seventh position in blue and mismatches in red. (B) Arrowhead indicates the shifted radiolabelled DNA. (C–E) Fuji BAS-2500 phosphorimages of quantitative EMSAs using increasing amount of His-*Tbx6*-DBD (range 0.21 nM–2.1 μM) or T-DBD (range: 4.0 μM–2.4 μM) added to a constant 10 pM of double-stranded labeled oligonucleotide corresponding to *Dll1*-*msd* BS1 or BS2. Percentage DNA bound versus concentration of protein was plotted and fitted to a three-parameter Hill equation to determine binding affinity (K<sub>d</sub>), Hill co-efficient, and maximum percentage bound (Max).

and BS2 (Fig. 1B). The T-DBD could also shift both BS1 and BS2, however, shifting of BS1 appeared less effective (Fig. 1B). To determine the binding affinities of the T- and Tbx6-DBDs for BS1 and BS2 we used a quantitative EMSA approach whereby increasing amounts of the Tbx6-DBD or T-DBD were added to a constant, limiting amount of radiolabeled BS1-4 (Fig. 1C–E). Because the DNA concentrations were negligible compared to the protein, the protein concentration required to bind half the DNA was taken as an approximation of the dissociation constant,  $K_d$  (Harada et al., 1994). The  $K_d$ 's of Tbx6-DBD for BS1 and BS2 were similar, at 1.53  $\mu$ M and 1.30  $\mu$ M, respectively. The T-DBD had a tenfold lower affinity for BS2, with a  $K_d$  of 13.88  $\mu$ M. The binding affinity of T-DBD for BS1 could not be measured, as our protein preparation did not allow for high enough concentrations to achieve enough data points to fit to a curve. The Hill co-efficient of Tbx6-DBD was 2.97 and 3.18 at BS1 and BS2, respectively, and 14.42 for T-DBD at BS2. Strong cooperativity was observed for both Tbx6-DBD and T-DBD, as determined by a Hill co-efficient value greater than one. These results demonstrate that T has a lower affinity for the T-box BSs found in the *Dll1-msd* enhancer.

### T and Tbx6 transcriptional activities at synthetic and endogenous enhancers

Given these differences in the binding affinities of T and Tbx6 for the sites with the *Dll1* enhancer, we next wanted to compare their transcriptional activities at several T-box enhancers, including the 24 bp palindromic T-bind site ( $T^{bind}$ ), a ~200 bp region of the *Dll1-msd* enhancer (*Dll1-msd*), and a ~300 bp promoter/enhancer region of *Mesp2* (*Mesp2-P/E*) each cloned upstream of a minimal promoter-luciferase (-luc). Both the *Dll1-msd* and *Mesp2-P/E* enhancers contain four putative T-box binding sites (Fig. 2) (White and Chapman, 2005; Yasuhiko et al., 2006, 2008). We generated N-terminal myc-tagged full-length T and Tbx6 expression constructs to characterize the activity of T and Tbx6 at these enhancers.  $T^{bind}$ -luc co-transfected into HEK293T cells with equivalent amounts of myc-Tbx6 or myc-T plasmids revealed that both myc-T and myc-Tbx6 activate transcription weakly from this enhancer, approximately 5.8- and 7.5-fold over background, respectively (Table 1).

The four T-box binding sites in the *Dll1-msd* enhancer are clustered within a 100 bp region. As confirmed by our binding affinities results, BS1 and BS2 match the Tbx6 consensus site, while only one matches the T consensus (Fig. 2). *Mesp2* is a confirmed downstream target of Tbx6, and is expressed in the anterior portion of the PSM (Yasuhiko et al., 2006). *Mesp2-P/E* contains four putative T-box binding sites within 300 bp upstream of the start of transcription and the endogenous promoter sequences (Fig. 2). Two of these sites match both the T and Tbx6 consensus binding sites (sites D and G from Yasuhiko et al., 2008), while the other two are found in a palindromic-like configuration (site B) that contains mismatches compared to the T and Tbx6 consensus sites. At least two of the sites (B, D or G) are required for expression in transgenic embryos and for Tbx6 activation in luciferase assays (Yasuhiko et al., 2008). Contrary to the T-bind synthetic enhancer results, myc-T and myc-Tbx6 activated at different levels from the *Dll1-msd* and *Mesp2-P/E* endogenous enhancers, with myc-Tbx6 consistently activating tenfold higher than myc-T (Table 1 and Fig. 2).

For each of the luciferase reporters we further tested whether we could detect evidence of competition between T and Tbx6. For these experiments, we performed luciferase assays transfecting a constant amount of the myc-Tbx6 expression plasmid with increasing amounts of myc-T expression plasmid. Because the levels of activation from the  $T^{bind}$ -luc were not statistically different when

myc-T or myc-Tbx6 were added separately, we predicted that we would not see a change in relative luciferase units (RLUs) with increasing levels of myc-T. As predicted, the addition of increasing amounts of myc-T to a steady amount of myc-Tbx6 for the  $T^{bind}$ -luc were not statistically different from Tbx6 alone until the highest levels of myc-T (25–50 ng) were added to a constant amount of myc-Tbx6 (25 ng). As previously described, we observed a tenfold difference in T versus Tbx6 transcriptional activity at the *Dll1-msd* and *Mesp2-P/E* enhancers when myc-T and myc-Tbx6 expression plasmids were used separately (Fig. 2C,D). We therefore hypothesized that if myc-T could compete with myc-Tbx6 at these enhancers then increasing the amount of myc-T relative to a constant amount of myc-Tbx6 would reduce the RLUs. In these experiments, we observed a statistically significant decrease in RLUs with increasing amounts of myc-T for *Dll1-msd-luc* (Fig. 2C). Less robust results were observed at *Mesp2-P/E*, for which statistically significant differences were only occasionally detected with the addition of myc-T, but this did not always correlate with the higher amounts of myc-T added (Fig. 2D). We next tested whether the DNA binding domain was necessary for competition by constructing myc-tagged full-length T and Tbx6 expression constructs that contain a single point mutation in the respective DBD, designated  $T^{R69W}$  and  $Tbx6^{R118W}$ . The point mutation changes a highly conserved arginine (polar amino acid) to a tryptophan (non-polar). This arginine makes polar interactions with DNA (Müller and Herrmann, 1997) and therefore a change from a charged to a non-polar amino acid is predicted to interfere with DNA binding. Mutations at the corresponding site in *Drosophila* T-box factor Omb fails to bind DNA (Sen et al., 2010). As predicted, the DBD mutants failed to activate or repress transcription in luciferase assays when used alone and did not compete when added with the converse wild-type T or Tbx6 (Fig. 2D,E). These results confirm that an intact and functional DBD, the T-domain, is required for competition between T-box factors in transcriptional assays.

### Upregulation of Tbx6 leads to T-like phenotypes

In mice, homozygous loss of *Tbx6* results in the mis-patterning of anterior somites, the formation of ectopic neural tubes at the expense of posterior somites, an enlarged tailbud and embryonic lethality by e12.5 (Chapman and Papaioannou, 1998). Approximately half of *Tbx6* heterozygous embryos display defects in the formation of the atlas and axis, while a quarter have defects in 1–2 sacral vertebrae (Sparrow et al., 2013). The *Tbx6* hypomorphic mutation, *rib-vertebrae* ( $Tbx6^{rv}$ ), is a mutation in the regulatory region of Tbx6 resulting in less than heterozygous levels of Tbx6 expression in  $Tbx6^{rv/rv}$  embryos and mice with fusions of ribs and vertebrae and a shortened axis (Watabe-Rudolph et al., 2002; White et al., 2003). To further explore the phenotypic consequences of altering *Tbx6* expression levels, we utilized our *Tbx6* transgenic line,  $Tbx6^{Tg46}$ , that harbors a transgene containing the entire *Tbx6* coding region along with upstream and downstream sequences required for proper temporal and spatial expression of *Tbx6* (White et al., 2005, 2003). The *Tg46* transgene expresses *Tbx6* RNA at lower than heterozygous levels and thus fails to rescue the *Tbx6* mutant phenotype;  $Tbx6^{-/-}$   $Tbx6^{Tg46/+}$  embryos display fusions of vertebrae and ribs similar to the *Tbx6* hypomorph,  $Tbx6^{rv/rv}$  (White et al., 2003). Embryos hemizygous for the *Tg46* transgene ( $Tbx6^{Tg46/+}$ ) on a wild-type background are phenotypically normal, except for an occasional (~5%) kinked tail. We tested the consequence of increasing the level of Tbx6 by homozygosing the *Tg46* transgene. Interestingly,  $Tbx6^{Tg46/Tg46}$  embryos have severely

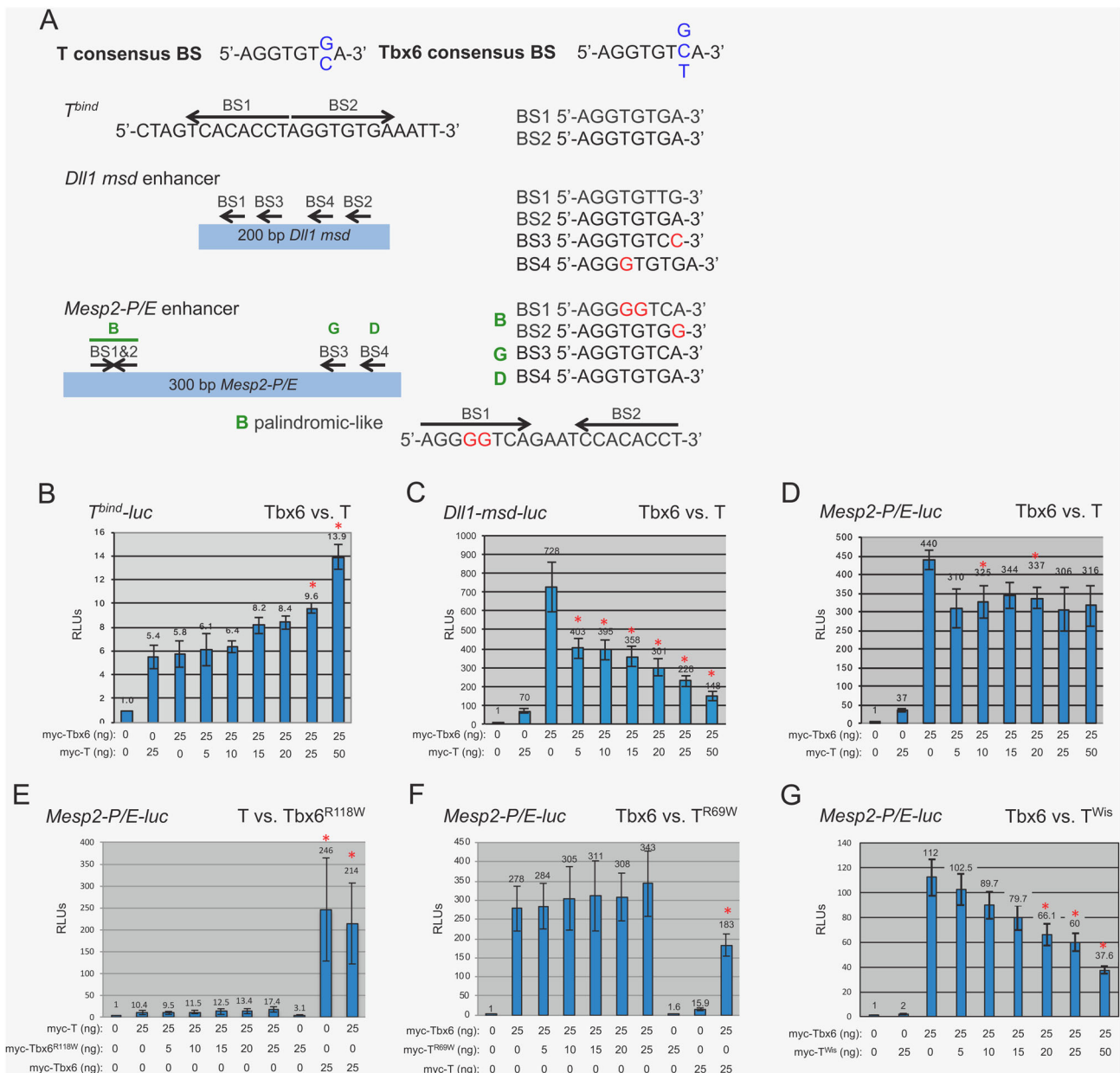


**Fig. 2. Luciferase assays.** (A) Graphical representations of the enhancers used for luciferase assays with the T and Tbx6 consensus binding sites and the T-box binding sites found within the enhancers. Mismatches are denoted in red. (B–G) Graphical analyses of relative luciferase units (RLUs) produced from transfecting the specified amount of the protein expression vector(s) with either the (B) *T<sup>bind</sup>-luc*, (C) *Dll1-msd-luc*, or (D–G) *Mesp2-P/E-luc* reporter vector. Empty protein expression vector served as a negative control and was set to 1. T<sup>R69W</sup> and Tbx6<sup>R118W</sup> are full-length proteins with a single amino acid change in the DBD. Competition luciferase assays were performed by adding increasing amounts of myc-T, myc-Tbx6, myc-T<sup>R69W</sup>, myc-Tbx6<sup>R118W</sup>, or myc-T<sup>Wis</sup> to a constant amount of myc-Tbx6 or myc-T, as indicated. Red asterisks above bars indicate  $P < 0.05$ .

truncated axes that terminate in a filamentous tail structure, with malformed or absent vertebrae in the filamentous tail regions (Fig. 3B,C). The small tail phenotype is noticeable by e9.5–e10.5, with tailbuds expressing lower levels of *T* suggesting a loss of progenitor cells necessary for caudal extension (Fig. S1D). By e15.5, these *Tbx6<sup>Tg46/Tg46</sup>* embryos are noticeably smaller than wild type and their hemizygous littermates with a high proportion dying perinatally for unknown reasons as all of the organs appear normal (Fig. 3A–C). In addition to the previously published consequences of under-expressing Tbx6 (Watabe-Rudolph et al., 2002; White et al., 2003), the above results show that there are also phenotypic consequences for over-expressing *Tbx6*.

### Tbx6 protein levels vary in different genetic backgrounds

Western blot analysis was used to quantitate Tbx6 protein levels in e10.5 tailbuds from *Tbx6<sup>rv/rv</sup>*, *Tbx6<sup>+/-</sup>*, and *Tbx6<sup>Tg46/Tg46</sup>* embryos, in addition to their respective wild-type background strains (Fig. S1). Interestingly, Tbx6 levels varied among the different background strains: C57Bl6/J (*Tbx6<sup>rv/rv</sup>* background) had the lowest levels of Tbx6 protein, followed by mixed C57Bl6/J/129SvEv (*Tbx6<sup>+/-</sup>* background) and finally FVB/N (*Tbx6<sup>Tg46/Tg46</sup>* background) had the most. Tbx6 protein levels were also variable among the different genotypes: *Tbx6<sup>rv/rv</sup>* tailbuds expressed the lowest, followed by a slight increase in *Tbx6<sup>+/-</sup>* tailbuds, and the greatest amount in *Tbx6<sup>Tg46/Tg46</sup>* tailbuds (Fig. S1). One caveat of



filamentous tail stub (Fig. 2I). The  $T^{Wis}$  mutation truncates the T protein in a regulatory domain required for its activity but leaves the DBD intact, thus  $T^{Wis}$  is believed to be a neomorph, generating phenotypes more severe than the null allele;  $T^{Wis}/T^{Wis}$  embryos produce no somites, while the  $T/T$  embryos can generate up to nine anterior somites (Conlon et al., 1995; Herrmann and Kispert, 1994; Herrmann et al., 1990; Kispert and Herrmann, 1994; Shedlovsky et al., 1988). Like the  $T$  null, the  $T^{Wis}$  mutation is epistatic to  $Tbx6$  (Chapman et al., 2003). The more severe  $T^{Wis}/T^{Wis}$  phenotype compared to that of the  $T/T$  (null allele) led to the hypothesis that the  $T^{Wis}$  protein blocks a related protein from binding the same DNA site(s) thus affecting transcription of target genes (Conlon et al., 1995; Herrmann and Kispert, 1994; Kispert and Herrmann, 1994). *Eomesodermin* and *Tbx6* are both co-expressed with T and are therefore candidates for this related protein (Arnold et al., 2008; Chapman et al., 1996; Russ et al., 2000). Here we genetically test whether  $T^{Wis}$  is interfering with Tbx6 function, by generating *Tbx6*  $T^{Wis}$  double heterozygous embryos ( $Tbx6^{+/-} T^{Wis}/+$ ), thus genetically reducing the amount of Tbx6 ( $Tbx6^{\pm/+/-}$ ) while expressing the  $T^{Wis}$  interfering protein ( $T^{Wis}/+$ ). To examine the phenotypes, we performed stains using Alcian Blue (cartilage) with or without Alizarin Red (ossified bone) of e15.5–17.5 skeletons. Indeed, eight out of fifteen  $Tbx6^{+/-} T^{Wis}/+$  embryos displayed fusions of several ribs and malformed vertebrae (Fig. 3K,M), resembling the *Tbx6* hypomorph,  $Tbx6^{rv/rv}$  (shown in Fig. 3G), while only one severely affected  $T^{Wis}/+$  embryo ( $n=10$ ) displayed rib fusions (Table 2). If rib fusions and vertebral abnormalities in  $T^{Wis}/+$   $Tbx6^{+/-}$  embryos are simply due to a loss of T protein function and not to a  $T^{Wis}$  blocking function, then embryos heterozygous for *Tbx6* in combination with the  $T$  null allele should have the same phenotype as the  $Tbx6^{+/-} T^{Wis}/+$  embryos. Instead, we found no rib fusions or vertebral malformations in  $Tbx6^{+/-} T/+$  embryonic skeletons ( $n=7$ ; Table 2). This phenotypic effect of  $T^{Wis}$  was specific to *Tbx6* as neither *wnt3a* nor *Dll1*, two genes functioning in this pathway (Dunty et al., 2008), had this effect when combined with  $T^{Wis}$  (Table 2). These results suggest that  $T^{Wis}$  specifically blocks Tbx6 function. Using luciferase assays we further show that while  $T^{Wis}$  itself has no activation or repressive activity at *Mesp2-P/E-luc*, it can decrease the RLUs when

increasing amounts of  $T^{Wis}$  expression plasmids are co-transfected with a constant level of *Tbx6* expression plasmid (Fig. 2G).

### Tbx6 cannot functionally replace T

While T and Tbx6 share similarities within the DBD and can bind similar sequences *in vitro* our current results show that they have different affinities for these binding sites, which may account for their differential activity in luciferase assays. Nevertheless, these factors can compete *in vitro* with competition being dependent on their T-domain, suggesting that they could have some redundant functions. Data from our lab along with others indicate at least some non-redundant functions. In  $T/T$  embryos, *Tbx6* is initially expressed, however, a mutant phenotype is evident by the time *Tbx6* expression is lost (Chapman et al., 1996). In *Tbx6* mutants, T expression is maintained in the bulbous tailbud, but this tissue does not form PAM (Chapman and Papaioannou, 1998). Thus, neither Tbx6 nor T appears to compensate for a loss of the other. However, this inability to compensate may simply be due to the level of T/Tbx6 protein expressed in mutant embryos. To further understand how similar or different T and Tbx6 function *in vivo* we undertook a knockin strategy in mice. The full-length *Tbx6* cDNA along with an IRES-nuclear localized *LacZ* and floxed *neo* selection cassette was knocked into the  $T$  locus at the initiating methionine (allele denoted  $T^{Tbx6ki}$ , Fig. 4A). Two of the correctly targeted ES cells were injected into C57Bl6/J blastocysts and chimeric mice ( $n=30$ ) were obtained. Interestingly, the chimeric mice obtained showed a low contribution from the ES cells as determined by coat color. One chimera with approximately 30–40% contribution from the ES cells had a short, kinky tail and shortened trunk compared to non-chimeric and low percentage chimeric littermates (Fig. 4C versus B). To determine whether high percentage chimeras were dying during embryogenesis we dissected chimeric embryos at e9.5. Chimeric embryos showed  $\beta$ -galactosidase activity in the notochord and tailbud in a T-specific manner, demonstrating that the knockin did not disrupt proper spatial expression from the  $T$  locus (Fig. 4D,E). However, abnormal phenotypes, including malformed somites and shortened axes, were observed in chimeric embryos (Fig. 4F). To correlate the ES cell contribution with the observed phenotypes, we injected  $T^{Tbx6ki/+}$  ES cells into blastocysts ubiquitously expressing GFP and transferred the embryos to recipient females to allow for further development. Embryos were dissected at e9.5, stained for  $\beta$ -galactosidase activity and imaged embryos using both bright field and fluorescent microscopy. Increased ES cell contribution corresponded to lower GFP signal. Chimeric embryos with low to medium contribution had defects in tailbud morphology, which was often blunt and edemic, with higher ES cell contributions resulting in abnormally-shaped somites (Fig. 4G–I). Finally, embryos with the highest contribution were lethal at this stage; embryos failed to turn and had truncated axes (Fig. 4J). Therefore high contributions by  $T^{Tbx6ki/+}$  ES cells that have only one functional copy of the  $T$  gene and express ectopic *Tbx6* in a T-specific manner lead to phenotypes indicative of disruption of PS function and somite formation. These embryonic defects presumably lead to the shortened axis and the kinked tail in the live born chimera (shown in Fig. 4C). These results suggest not only that Tbx6 cannot functionally replace T, but also that the levels of T and Tbx6 must be tightly regulated for proper mesoderm formation.

**Table 2. Rib and vertebral phenotypes in T and  $T^{Wis}$  embryos in combination with *Tbx6*, *wnt3a* or *Dll1***

Genotype	Phenotype		<i>n</i>
	Rib/vertebral fusions	Normal ribs/vertebrae	
$T/+ Tbx6^{+/-}$	0	7	7
$T/+ Tbx6^{+/+}$	0	7	7
$T^{Wis}/+ Tbx6^{+/-}$	8	7	15
$T^{Wis}/+ Tbx6^{+/+}$	1	9	10
$T/+ wnt3a^{+/-}$	0	4	4
$T/+ wnt3a^{+/+}$	0	3	3
$T^{Wis}/+ wnt3a^{+/-}$	0	9	9
$T^{Wis}/+ wnt3a^{+/+}$	0	10	10
$+/+ Dll1^{+/-}$	5*	7	12
$T/+ Dll1^{+/-}$	2*	7	9
$T/+ Dll1^{+/+}$	0	10	10
$T^{Wis}/+ Dll1^{+/-}$	0	11	11
$T^{Wis}/+ Dll1^{+/+}$	0	5	5

Rib/vertebral fusion phenotypes were observed in approximately half of the  $T^{Wis}/+ Tbx6^{+/-}$  embryos, while there was no similar interaction with the  $T$  null allele. The absence of a more severe phenotype in compound  $T^{Wis}/+ wnt3a^{+/-}$  or  $T^{Wis}/+ Dll1^{+/-}$  further supports the specificity of the genetic interaction of  $T^{Wis}$  with *Tbx6*.

### DISCUSSION

T and Tbx6 are co-expressed in the primitive streak in addition to their unique areas of expression, T in the notochord and *Tbx6* in the

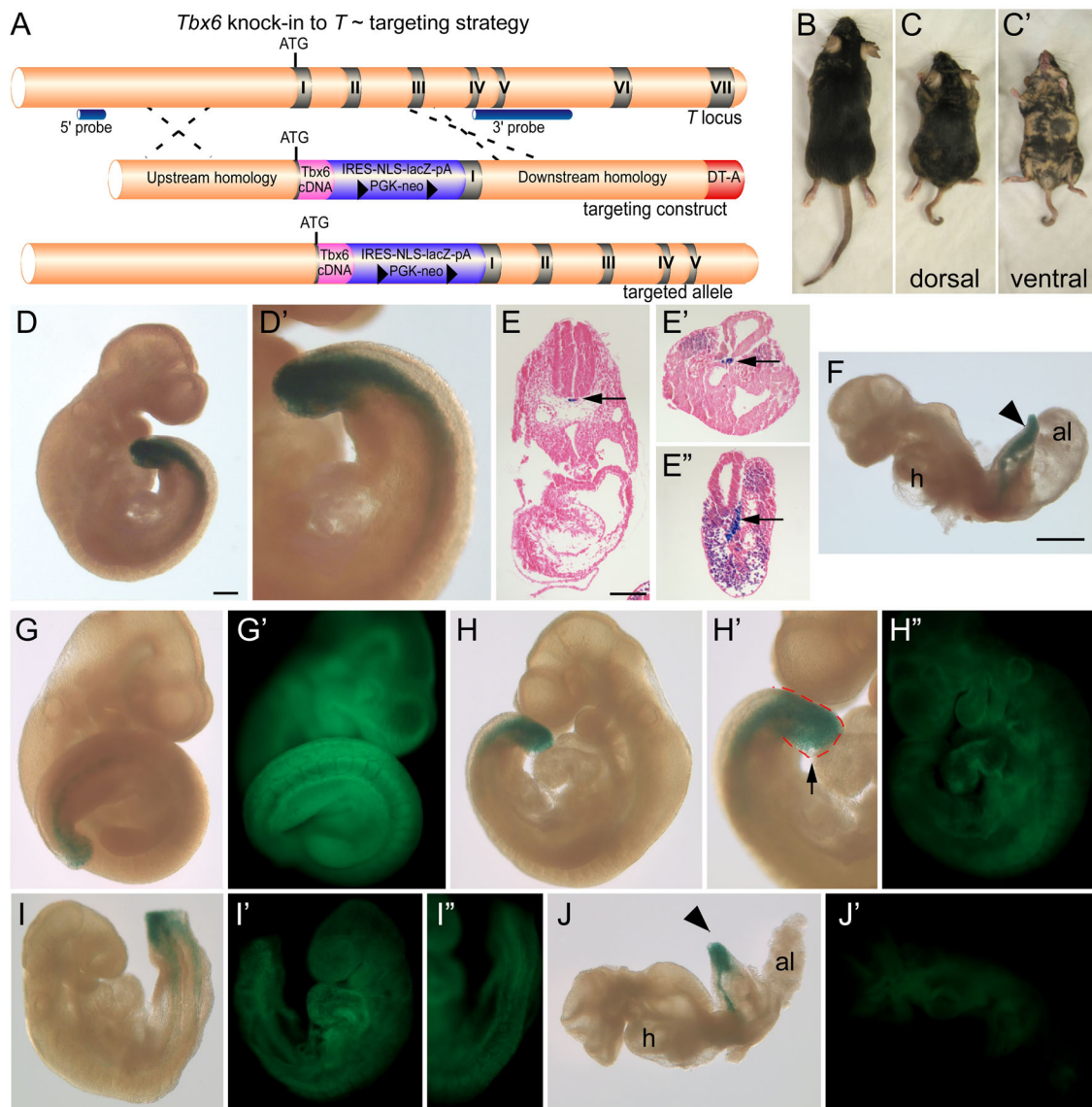


**Fig. 4. *Tbx6* knock-in *T* targeting strategy and chimera phenotypes.** (A) Schematic of the targeting strategy to knock the *Tbx6* cDNA into the *T* locus at the initiating methionine  $T^{Tbx6ki}$ . The positions of the IRES-lacZ-PGK-neo positive selection cassette, the diphtheria toxin A (DT-A) negative selection cassette, and 5' and 3' external probes for genotyping are indicated. (B,C) Dorsal views of littermate chimeric mice derived from injecting  $T^{Tbx6ki+}$  ES cells into C57 blastocysts. Mice in panels B and C represent ~10% and 40% chimerism, respectively. (C') Ventral view of chimera shown in panel C. Note the short axis and kinky tail of the higher percentage chimera (panel C) compared to its littermate (panel B). (D,D')  $\beta$ -galactosidase staining of a chimeric embryo and representative sections (E–E') showing the presence of the *lacZ* reporter activity in the PS and notochord (arrow), indicative of the *T* expression domains. (G–J) Chimeric embryos resulting from  $T^{Tbx6ki+}$  ES cell injections into GFP-expressing blastocysts were stained for  $\beta$ -galactosidase activity and imaged in bright field and GFP fluorescence (G'–J'). Panels G to J represent low (panel G,G') to high percentage (panel J,J') contribution of the  $T^{Tbx6ki+}$  ES cells in chimeric embryos as shown by reduced GFP from panels G' to J'. Developmental defects include abnormal tail and somite morphology (H,I) and shortened axis and failure to turn (J) in the higher percentage chimeras. Magnification bars represent 200  $\mu$ m (D,G–I), 150  $\mu$ m (E), 700  $\mu$ m (F,J).

presomitic mesoderm. Both *T* and *Tbx6* are also thought to be transcriptional activators and to regulate at least one common target, *Dll1* (Hofmann et al., 2004; White and Chapman, 2005; Yasuhiko et al., 2006, 2008). Here we sought to understand how similar or different these related T-box transcription factors function *in vitro* and *in vivo*. Because *T* and *Tbx6* can bind to very similar sequences and both can activate gene expression, we asked whether they are interchangeable if they are expressed in the correct places and times.

We tested the *in vitro* transcriptional activity of *T* and *Tbx6* at a synthetic ( $T^{bind}$ ) enhancer. Approximately equal levels of activation by *Tbx6* and *T* at the  $T^{bind}$  enhancer was not surprising, as both *T* and *Tbx6* have previously been shown to bind to this element with *T*

binding as a dimer across the two half-sites and *Tbx6* binding as two monomers to the two half-sites (Kispert and Herrmann, 1993; Müller and Herrmann, 1997; White and Chapman, 2005). Both *T* and *Tbx6* regulate *Dll1* expression (Hofmann et al., 2004; White and Chapman, 2005). Here we show that while both *T* and *Tbx6* can activate transcription from the *Dll1*-*msd* enhancer *in vitro*, *Tbx6* serves as a better transcriptional activator. We further tested a second endogenous enhancer, *Mesp2*-*P/E*. Similar to results with the *Dll1*-*msd* enhancer, *Tbx6* activated transcription at a tenfold higher level than *T*. As demonstrated by chromatin immunoprecipitation (ChIP), *Mesp2* is a confirmed *Tbx6* target (Yasuhiko et al., 2006). Although myc-*T* can activate the *Mesp2*-*P/E*

enhancer *in vitro*, it is unlikely that it reflects a physiologically relevant event, since *T* is not expressed in the anterior PSM where *Mesp2* expression overlaps with *Tbx6*. However, it is possible that instead of activating, *T* may bind the *Mesp2* enhancer in the PS/tailbud and here serves to block *Tbx6* from binding, thus repressing *Mesp2* transcription. This possibility would need to be verified by ChIP experiments. Differential activation of the *Dll1-msd* and *Mesp2-P/E* enhancers by *T* and *Tbx6* can occur for several reasons that are not necessarily mutually exclusive. *Tbx6* may simply be a stronger activator of transcription than *T*. Alternatively, *T* may require a co-factor(s) for more robust activity and this co-factor(s) may not be expressed in the HEK293T cells that were used for luciferase assays. Indeed, others have shown that both *T* and *Tbx6* can synergize with the canonical Wnt signaling pathway to regulate *Dll1* expression (Hofmann et al., 2004). The tenfold difference in their activities at these endogenous enhancers, allowed us to test the hypothesis that *T* and *Tbx6* can compete at target gene enhancers. In these experiments, increasing the amount of *T*, while *Tbx6* levels remained constant, resulted in a significant decrease in transcriptional activity, most noticeable using the common *Dll1* target. We showed that this competition requires a functional DNA binding domain by using expression constructs that coded for full-length *T* and *Tbx6* proteins, but which had a single point mutation in the DBD that is predicted to interfere with DNA binding. While these studies support that *T* and *Tbx6* are competing at the level of DNA binding sites, rather than competing for co-factors in these assays, it is possible that the point mutations interfere with binding to an unknown co-factor(s). The truncated  $T^{Wis}$  protein that retains a functional DBD but does not itself activate or repress transcription in these luciferase assays could still compete with *Tbx6* further supporting our *in vivo* genetic data.

Although we did not test the importance of the individual T-box BSs in our luciferase assays, we did measure the binding affinities of *T* and *Tbx6* at two sites within the *Dll1-msd* enhancer. We first found that both *T* and *Tbx6* can shift two (BS1 and BS2) of the four BSs, but that *T* shifted BS1 less effectively than BS2. Quantitative EMSAs confirmed these findings and that *Tbx6* bound to both BS1 and BS2 at approximately the same affinity, which for BS2 was tenfold higher than *T*'s binding affinity. We could not measure the affinity of *T* for BS1 because it was too low at the concentrations of proteins used. These differences in *T* and *Tbx6* affinities are consistent with the binding site preferences identified for *T* and *Tbx6* using binding site selection assays (Kispert and Herrmann, 1993; White and Chapman, 2005). For example, *Dll1-msd* BS1 has a *T* in the seventh position just outside the core AGGTGT. Binding site selections revealed only a *G* or *C* at this position for *T*, while *G*, *C*, or *T* was preferred for *Tbx6*. Interestingly, our quantitative EMSAs revealed *Tbx6* had a tenfold higher affinity than *T* at BS2, for which binding site selection experiments showed that both *T* and *Tbx6* could bind the site. Preferences of *T* and *Tbx6* for multiple BSs in specific arrangements, for example in a palindromic orientation as was originally identified for the *T* dimer (Müller and Herrmann, 1997), may contribute to the differences found in affinity for BS2. The identification of additional *T* and *Tbx6* targets by ChIP would be needed to further explore this possibility. These differences in binding affinities of *T* and *Tbx6* to the sites in the *Dll1-msd* enhancer may contribute to their differential transcriptional activities found *in vitro*.

Because *T* and *Tbx6* can compete *in vitro*, we were curious whether this also occurs *in vivo* and used a variety of transgenic mice to explore this possibility. We observed axis truncation and tail dysmorphology phenotypes in the *Tbx6<sup>Tg46/Tg46</sup>* embryos, which

express greater than wild-type levels of *Tbx6* in its endogenous domains, i.e. the PS and presomitic mesoderm. This result suggested that increased levels of *Tbx6* interfere with the function of another T-box protein, with *T* being a likely candidate as it is required for axis elongation and the similarities of *Tbx6<sup>Tg46/Tg46</sup>* and *T* heterozygotes. Alternatively, overexpression of *Tbx6* may simply drive higher levels of a downstream target(s) and this then interferes with normal axis formation. Our genetic studies utilizing the  $T^{Wis}$  allele revealed a genetic interaction with *Tbx6* in double heterozygous embryos, specifically fusions and malformations of ribs and vertebrae. Interestingly these same phenotypes were not observed in *Tbx6*; *T* null allele double heterozygotes, nor were similar phenotypes observed in embryos double heterozygous for  $T^{Wis}$  and either *wnt3a* or *Dll1*, two other genes functioning in the PS to presomitic mesoderm pathway. These results suggest that the truncated  $T^{Wis}$  protein, which contains an intact DBD, can interfere specifically with *Tbx6* function in the developing embryo. This is supported by our observation that  $T^{Wis/+}$ , *Tbx6<sup>+/-</sup>* embryos share similarities with *Tbx6<sup>rv/rv</sup>* embryos (hypomorphic allele) that expresses lower than heterozygous levels of *Tbx6*. Together these results suggest that the  $T^{Wis}$  protein can specifically block *Tbx6* function. Future RNA-seq experiments to examine changes in gene expression in these different genetic contexts could lead to a better understanding of the exact mechanism underlying these phenotypes. In addition, quantitative ChIP experiments to measure changes in *T* and *Tbx6* occupancy at target genes in these different genetic contexts would show how co-expressed T-box proteins interact at the genome level. Nevertheless, our results indicate that over- or under-expression of *Tbx6* leads to the abnormal formation of axial structures, specifically ribs and vertebrae.

Finally, we tested whether *T* and *Tbx6* were functionally interchangeable by replacing *T* with *Tbx6* in the developing mouse embryos. Despite the T-domains of these proteins sharing 53% identity and both being transcriptional activators, *Tbx6* could not compensate for the single loss of *T* even in chimeras. In fact, high percentage chimeric embryos containing  $T^{Tbx6ki}$  heterozygous cells share similarities with *T* null embryos, including truncated axes and malformed somites. This result indicates that *T* and *Tbx6* behave differently, which could occur simply through differences in their preferences for binding sites in target genes, transcriptional activity, or a combination of the two. However, due to the severity of phenotypes in chimeric embryos using  $T^{Tbx6ki}$  heterozygous cells, which resembled *T* null rather than *T* heterozygous phenotypes, we favor instead that there is some level of competition between the related factors. This competition is supported by our additional genetic studies that showed increasing *Tbx6* levels using our *Tg46* transgene generates T-like phenotypes while genetic studies using the dominant *T* allele,  $T^{Wis}$ , appears to compete with *Tbx6*. Altogether, these results suggest that controlling both the localization and the levels of these related transcription factors is critical for normal development.

## MATERIALS AND METHODS

### T6 and T DBD cloning and expression

The DBD region of *T* and *Tbx6* [*T*: amino acids (aa) 41-224; *Tbx6*: aa 90-277] were PCR amplified and cloned into the PET151/D-TOPO (Invitrogen) producing a Histidine-tagged fusion protein. Transformed bacterial cultures were auto-induced, lysed and His-tagged fusion proteins were purified using nickel affinity purification followed by TEV protease digestion and a second round of nickel affinity purification to remove the Histidine tag. The protein was then further purified via anion exchange and size exclusion chromatography. Limited trypsin proteolysis revealed that >90% of isolated, purified proteins were correctly folded.

## EMSAs

Oligonucleotides were end-labeled with  $\gamma$ -<sup>32</sup>P-ATP using T4 polynucleotide kinase. Oligonucleotides were annealed and purified using Micro Bio-Spin P-30 Tris purification columns (Bio-Rad). The percentage of double-stranded versus single-stranded probe was determined with the percentage of double-stranded probe recovered being greater than 85% in all cases. Subsequently, the percentage of double-stranded probe for each experiment was standardized so equivalent amounts were used. All EMSA binding reactions were prepared in a final reaction volume of 10  $\mu$ l in BBT buffer (25 mM HEPES pH 7.4, 75 mM NaCl, 1 mM DTT, 0.25 mM EDTA, 0.1% NP-40, 1 mM MgCl<sub>2</sub>, 10% glycerol, 10  $\mu$ g/ml BSA). 0.1 mg/ml Poly dI-dC was added as a non-specific competitor. Binding reactions were incubated at room temperature for 20 min and loading on 4–6% non-denaturing PAGE (37.5:1) run in 1 $\times$  TAE. Gels were dried unfixed, exposed to a phosphoimager screen and imaged on a Fuji BAS-2500 Phosphoimager. Oligonucleotides used: (bold letters indicate core T-box binding sequence) *T<sup>bind</sup>*: 5'-CTAGT-CACACCTAGGTGTGAAATT-3' *Dll1BS1*: 5'-TCACTGTAGGTGTTG-CTGTCCTGT-3' *Dll1BS2*: 5'-TCCCGAGGTGTGA-TTCTTGA-3' *Dll1BS3*: 5'-GTGGATCCAGGTGTCTCACTGGGCTGC-3' *Dll1BS4*: 5'-TGGATCCTAGGGTGTACCTGACGGCTGC-3'

For quantitation, reactions were prepared as described above, except that increasing amounts of Tbx6-DBD (range:  $2.1 \times 10^{-8}$ – $2.1 \times 10^{-5}$  M) or T-DBD (range:  $4.0 \times 10^{-6}$ – $2.4 \times 10^{-5}$  M) were added to a constant, limiting amount of labeled *Dll1 BS1-4* oligonucleotides (10 pM) and incubated one hour at room temperature to ensure reactions were at equilibrium. Reactions were run on a 6% non-denaturing PAGE. Quantitation was performed as previously described (Harada et al., 1994). Briefly, the amount of free and bound DNA was quantitated using a Fuji BAS-2500 phosphoimager and analysis with ImageGauge software. Percentage of bound DNA was determined by the following formula: (Shifted DNA)/(Shifted DNA+Free DNA). The concentration of Tbx6-DBD or T-DBD was plotted versus the percentage of DNA bound. The data was fit to a three-parameter Hill equation using SigmaPlot software (equation:  $y = ax^b / (c^b + x^b)$ , where a=the maximum value of y (percent bound), b=the Hill co-efficient, and c= $K_d$ ).

## Plasmid constructs

Full-length *Tbx6* and *T* cDNAs were cloned in-frame with the N-terminal myc-epitope tag of the mammalian pCS expression vectors (Wehn and Chapman, 2010). To generate point mutations in the T and Tbx6 DBDs, we modified these pCS-myc-Tbx6 and -T expression vectors to change an arginine in the T-domain to a tryptophan (Tbx6<sup>R118W</sup> and T<sup>R69W</sup>) using the QuikChange kit (Stratagene) following the manufacturer's instructions. To generate the truncated T<sup>Wis</sup> protein, the region of the *T* cDNA encoding the first 345 amino acids was PCR amplified and cloned in-frame with the N-terminal myc-epitope tag of the pCS expression vector. The luciferase reporter vectors were all constructed in pGL4.10[luc] (Promega) except that a putative T-box binding site within the vector was changed (pGL4M- $\beta$ -globin-luciferase). Enhancers included the 24 bp palindromic T-bind element, a ~200 bp region of the *Dll1-msd* enhancer (*Dll1-msd-luc*) and a ~300 bp region of the *Mesp2* promoter/enhancer (*Mesp2-P/E-luc*), which were cloned upstream of the  $\beta$ -globin minimal promoter-luciferase (Kispert and Herrmann, 1993; White and Chapman, 2005; Yasuhiko et al., 2006).

## Luciferase assays

HEK293T cells were chosen for luciferase assays because of their reliable transfection rate and their use for assaying transcriptional activity for multiple T-box proteins (Brown et al., 2005; Wehn and Chapman, 2010).  $1 \times 10^5$  HEK293T cells were plated per well in tissue culture-treated 96-well dishes, and transfected with Lipofectamine 2000 (Invitrogen) in suspension. 10 ng of the designated luciferase reporter plasmid was transfected per well along with 1 ng of *pRenilla Luciferase-CMV*, which served as an internal control. The amount of plasmid encoding myc-epitope tagged Tbx6, T, Tbx6<sup>R118W</sup>, T<sup>R69W</sup> or T<sup>Wis</sup> were as indicated, and empty pCS vector was added as necessary to maintain the same amounts of transfected DNA constant between samples. Twenty-four hours after transfection, cells were processed with Dual Glo luciferase reagent (Promega) according to the manufacturer's directions, and the intensity measured on a Berthold XS<sup>3</sup>

LB960 luminometer. Luciferase readings were normalized to the Renilla luciferase, and ratios were normalized to the luciferase plasmid transfected with an empty pCS3 expression vector control. Transfections were performed in triplicate in 96-well plates, and repeated at least once. Relative luciferase units (RLUs) and standard error were calculated over at least six data points. Statistical analyses were performed using one-way ANOVA tests.

## Mice

*Tbx6<sup>tm1Pa</sup>* (Chapman and Papaioannou, 1998), *Tg(Tbx6)46Dlc* (White et al., 2003), *T<sup>Wis</sup>* (Shedlovsky et al., 1988), *T* null (Kwan, Chapman, Behringer unpublished), *wnt3a<sup>TmlAmc</sup>* (Takada et al., 1994) and *Dll1<sup>TmlGos</sup>* (Hrabě de Angelis et al., 1997) were utilized for genetic crosses. JAX stock #004353 mice *C57BL/6-Tg(UBC-GFP)30Scha/J* (Schaefer et al., 2001) were used to generate GFP-expressing blastocysts. Animals were mated and checked daily for the presence of a copulation plug. Noon on the day of the plug was considered e0.5 days post-coitum. Females were euthanized and embryos dissected from e9.5 to e18.5. All animal work was performed in accordance with the guidelines established by the University of Pittsburgh's Institutional Animal Care and Use Committee.

## Skeletal preparations

Skeletons from e14.5 to e18.5 embryos were stained with Alcian Blue with or without co-staining with Alizarin Red as described by Nagy et al. (2003), except that the staining was performed at 37°C.

## Western blotting

Embryonic tailbud tissue was dissected at e10.5 or HEK293T cells were transfected with the specified expression plasmids and the tissues/cells were homogenized in RIPA buffer. Bradford dye assays were performed to determine total protein concentration, and equal amounts of protein were loaded onto 7.5% SDS-PAGE gels, transferred to nitrocellulose, and blotted with rabbit anti-Tbx6 (1:2500) (White and Chapman, 2005), anti-9E10 (anti-myc, 1:500, Sigma-Aldrich) or anti-actin (1:1000, Cytoskeleton) in blocking buffer (TBTT containing 5% non-fat dry milk), and subsequently incubated in anti-mouse or rabbit HRP-conjugated secondary antibody (1:2500, Jackson ImmunoResearch), followed by ECL (Amersham) with Kodak Image Station quantification.

## Whole-mount immunocytochemistry

Immunocytochemistry was performed as described in Nagy et al. (2003). The Tbx6 N-terminal affinity purified antibody was used at a 1:500 dilution (White and Chapman, 2005). Goat anti-rabbit:HRP-conjugated secondary antibody (Jackson ImmunoResearch) was used at a 1:500 dilution and staining was performed in the presence of DAB, hydrogen peroxide and nickel chloride.

## Whole-mount *in situ* hybridization

Whole-mount *in situ* hybridization was performed as previously described by Wilkinson (1992) using antisense riboprobes for *T*. Hybridization and washes were performed at 63°C.

## Gene targeting

The Tbx6 knockin to *T* targeting construct was made by inserting the *Tbx6* cDNA at the start codon of the *T* gene, using 4.8 and 4 kb upstream and downstream homology regions from the *T* genomic region. An IRES-*lacZ*-floxed PGK-neo cassette was inserted after the *Tbx6* cDNA and a diphtheria toxin A cassette was inserted 3' to the downstream homology for positive and negative selection, respectively. The linearized targeting construct was electroporated into R1 ES cells, selected and genotyped by Southern blot using 5' and 3' external probes according to standard techniques (Nagy et al., 2003).

## ES cell chimeras

Two of the targeted ES cell lines were injected into C57Bl6/J blastocysts or GFP-blastocysts, transferred to Swiss Webster pseudopregnant females, and allowed to develop *in vivo* either until birth ( $n=33$  live born chimeras generated) or until e9.5 according to standard techniques (Nagy et al., 2003).

Chimeric embryos ( $n=39$ ) were dissected, fixed and stained for  $\beta$ -galactosidase activity (Ciruna et al., 1997) and either sectioned at 8–10  $\mu\text{m}$  and co-stained with Eosin or imaged for GFP fluorescence.

#### Acknowledgements

We would like to thank Andrew VanDemark for assistance preparing recombinant proteins and advice on the binding affinity studies, Jeffrey Lawrence for experimental advice and Gerard Campbell for critical discussion and review of the manuscript. Results/Discussion in this paper are reproduced from the PhD theses of A.K.W. (University of Pittsburgh, 2010) and D.R.F. (University of Pittsburgh, 2010).

#### Competing interests

The authors declare no competing or financial interests.

#### Author contributions

Conceptualization: A.K.W., D.R.F., D.L.C.; Methodology: A.K.W., D.R.F., D.L.C.; Formal analysis: A.K.W., D.R.F., C.E.S., D.S., D.L.C.; Investigation: A.K.W., D.R.F., C.E.S., D.S., D.L.C.; Supervision: A.K.W., D.L.C.; Funding acquisition: D.L.C.

#### Funding

This work was supported by grants from the National Institutes of Health (NIH) [HD38786], the National Science Foundation (NSF) [IOS-1050189] and the University of Pittsburgh, Central Research Development Fund.

#### Supplementary information

Supplementary information available online at <https://bio.biologists.org/lookup/doi/10.1242/bio.054692.supplemental>

#### References

- Arnold, S. J., Hofmann, U. K., Bikoff, E. K. and Robertson, E. J. (2008). Pivotal roles for eomesodermin during axis formation, epithelium-to-mesenchyme transition and endoderm specification in the mouse. *Development* **135**, 501–511. doi:10.1242/dev.014357
- Beckers, J., Caron, A., Hrabě de Angelis, M., Hans, S., Campos-Ortega, J. A. and Gossler, A. (2000a). Distinct regulatory elements direct Delta1 expression in the nervous system and paraxial mesoderm of transgenic mice. *Mech. Dev.* **95**, 23–34. doi:10.1016/S0925-4773(00)00322-1
- Beckers, J., Schlautmann, N. and Gossler, A. (2000b). The mouse rib-vertebrae mutation disrupts anterior-posterior somite patterning and genetically interacts with a delta1 null allele. *Mech. Dev.* **95**, 35–46. doi:10.1016/S0925-4773(00)00323-3
- Beisaw, A., Tsaytler, P., Koch, F., Schmitz, S. U., Melissari, M. T., Senft, A. D., Wittler, L., Pennimpede, T., Macura, K., Herrmann, B. G. et al. (2018). BRACHYURY directs histone acetylation to target loci during mesoderm development. *EMBO Rep.* **19**, 118–134. doi:10.15252/embr.201744201
- Brown, D. D., Martz, S. N., Binder, O., Goetz, S. C., Price, B. M., Smith, J. C. and Conlon, F. L. (2005). Tbx5 and Tbx20 act synergistically to control vertebrate heart morphogenesis. *Development* **132**, 553–563. doi:10.1242/dev.01596
- Buckingham, K. J., McMillin, M. J., Braggiotti, M. M., Shively, K. M., Magnaye, K. M., Cortes, A., Weinmann, A. S., Lyons, L. A. and Bamshad, M. J. (2013). Multiple mutant T alleles cause haploinsufficiency of Brachyury and short tails in Manx cats. *Mamm. Genome* **24**, 400–408. doi:10.1007/s00335-013-9471-1
- Chapman, D. L. and Papaioannou, V. E. (1998). Three neural tubes in mouse embryos with mutations in the T-box gene Tbx6. *Nature* **391**, 695–697. doi:10.1038/35624
- Chapman, D. L., Agulnik, I., Hancock, S., Silver, L. M. and Papaioannou, V. E. (1996). Tbx6, a mouse T-box gene implicated in paraxial mesoderm formation at gastrulation. *Dev. Biol.* **180**, 534–542. doi:10.1006/dbio.1996.0326
- Chapman, D. L., Cooper-Morgan, A., Harrelson, Z. and Papaioannou, V. E. (2003). Critical role for Tbx6 in mesoderm specification in the mouse embryo. *Mech. Dev.* **120**, 837–847. doi:10.1016/S0925-4773(03)00066-2
- Ciruna, B. G., Schwartz, L., Harpal, K., Yamaguchi, T. P., Rossant, J. (1997). Chimeric analysis of fibroblast growth factor receptor-1 (Fgfr1) function: a role for FGFR1 in morphogenetic movement through the primitive streak. *Development* **124**, 2829–2841.
- Conlon, F. L., Wright, C. V. and Robertson, E. J. (1995). Effects of the  $T^{Wts}$  mutation on notochord formation and mesodermal patterning. *Mech. Dev.* **49**, 201–209. doi:10.1016/0925-4773(94)00318-H
- Dobrovolskaia-Zavadskaia, N. (1927). Sur la mortification spontanée de la queue chez la souris nouveau-née sur l'existence d'un caractère (facteur) héréditaire "non viable". *C R Seanc Soc Biol* **97**, 114–116.
- Dunty, W. C., Jr., Biris, K. K., Chalamalasetty, R. B., Taketo, M. M., Lewandoski, M. and Yamaguchi, T. P. (2008). Wnt3a/beta-catenin signaling controls posterior body development by coordinating mesoderm formation and segmentation. *Development* **135**, 85–94. doi:10.1242/dev.009266
- Ghosh, T. K., Brook, J. D. and Wilsdon, A. (2017). T-Box Genes in Human Development and Disease. *Curr. Top. Dev. Biol.* **122**, 383–415. doi:10.1016/bbs.ctdb.2016.08.006
- Harada, R., Dufort, D., Denis-Larose, C. and Nepveu, A. (1994). Conserved cut repeats in the human cut homeodomain protein function as DNA binding domains. *J. Biol. Chem.* **269**, 2062–2067.
- Haworth, K., Putt, W., Cattanach, B., Breen, M., Binns, M., Lingaas, F. and Edwards, Y. H. (2001). Canine homolog of the T-box transcription factor T; failure of the protein to bind to its DNA target leads to a short-tail phenotype. *Mamm. Genome* **12**, 212–218. doi:10.1007/s003350010253
- Herrmann, B. G. and Kispert, A. (1994). The T genes in embryogenesis. *Trends Genet.* **10**, 280–286. doi:10.1016/0168-9525(90)90011-T
- Herrmann, B. G., Labeit, S., Poustka, A., King, T. R. and Lehrach, H. (1990). Cloning of the T gene required in mesoderm formation in the mouse. *Nature* **343**, 617–622. doi:10.1038/343617a0
- Hofmann, M., Schuster-Gossler, K., Watabe-Rudolph, M., Aulehla, A., Herrmann, B. G. and Gossler, A. (2004). WNT signaling, in synergy with T/TBX6, controls Notch signaling by regulating Dll1 expression in the presomitic mesoderm of mouse embryos. *Genes Dev.* **18**, 2712–2717. doi:10.1101/gad.1248604
- Hrabě de Angelis, M., McIntyre, J., II and Gossler, A. (1997). Maintenance of somite borders in mice requires the Delta homologue Dll1. *Nature* **386**, 717–721. doi:10.1038/386717a0
- Istaces, N., Splittgerber, M., Lima Silva, V., Nguyen, M., Thomas, S., Le, A., Achouri, Y., Calonne, E., Defrance, M., Fuks, F. et al. (2019). EOMES interacts with RUNX3 and BRG1 to promote innate memory cell formation through epigenetic reprogramming. *Nat. Commun.* **10**, 3306. doi:10.1038/s41467-019-1233-6
- Kispert, A. and Herrmann, B. G. (1993). The Brachyury gene encodes a novel DNA binding protein. *EMBO J.* **12**, 3211–3220. doi:10.1002/j.1460-2075.1993.tb05990.x
- Kispert, A. and Herrmann, B. G. (1994). Immunohistochemical analysis of the Brachyury protein in wild-type and mutant mouse embryos. *Dev. Biol.* **161**, 179–193. doi:10.1006/dbio.1994.1019
- Lewis, M. D., Miller, S. A., Miazgowicz, M. M., Beima, K. M. and Weinmann, A. S. (2007). T-bet's ability to regulate individual target genes requires the conserved T-box domain to recruit histone methyltransferase activity and a separate family member-specific transactivation domain. *Mol. Cell. Biol.* **27**, 8510–8521. doi:10.1128/MCB.01615-07
- MacMurray, A. and Shin, H. S. (1988). The antimorphic nature of the Tc allele at the mouse T locus. *Genetics* **120**, 545–550.
- Miller, S. A., Huang, A. C., Miazgowicz, M. M., Brassil, M. M. and Weinmann, A. S. (2008). Coordinated but physically separable interaction with H3K27-demethylase and H3K4-methyltransferase activities are required for T-box protein-mediated activation of developmental gene expression. *Genes Dev.* **22**, 2980–2993. doi:10.1101/gad.1689708
- Miller, S. A., Mohn, S. E. and Weinmann, A. S. (2010). Jmjd3 and UTX play a demethylase-independent role in chromatin remodeling to regulate T-box family member-dependent gene expression. *Mol. Cell* **40**, 594–605. doi:10.1016/j.molcel.2010.10.028
- Müller, C. W. and Herrmann, B. G. (1997). Crystallographic structure of the T domain-DNA complex of the Brachyury transcription factor. *Nature* **389**, 884–888. doi:10.1038/39929
- Nagy, A., Rossant, J., Nagy, R., Abramow-Newerly, W. and Roder, J. C. (1993). Derivation of completely cell culture-derived mice from early-passage embryonic stem cells. *Proc. Natl. Acad. Sci. USA* **90**, 8424–8428. doi:10.1073/pnas.90.18.8424
- Nagy, A., Gertsenstein, M., Vintersten, K. and Behringer, R. R. (2003). *Manipulating the Mouse Embryo*, 3rd edn. Cold Spring Harbor: Cold Spring Harbor Laboratory Press.
- Papaioannou, V. E. (2014). The T-box gene family: emerging roles in development, stem cells and cancer. *Development* **141**, 3819–3833. doi:10.1242/dev.104471
- Russ, A. P., Wattler, S., Colledge, W. H., Aparicio, S. A. J. R., Carlton, M. B., Pearce, J. J., Barton, S. C., Surani, M. A., Ryan, K., Nehls, M. C. et al. (2000). Eomesodermin is required for mouse trophoblast development and mesoderm formation. *Nature* **404**, 95–99. doi:10.1038/35003601
- Schaefer, B. C., Schaefer, M. L., Kappler, J. W., Marrack, P. and Kedl, R. M. (2001). Observation of antigen-dependent CD8+ T-cell/ dendritic cell interactions in vivo. *Cell. Immunol.* **214**, 110–122. doi:10.1006/cimm.2001.1895
- Sen, A., Gadamski, C., Balles, J., Abassi, Y., Dorner, C. and Pflugfelder, G. O. (2010). Null mutations in Drosophila Optomotor-blind affect T-domain residues conserved in all Tbx proteins. *Molecular genetics and genomics : MGG* **283**, 147–156. doi:10.1007/s00438-009-0505-z
- Shedlovsky, A., King, T. R. and Dove, W. F. (1988). Saturation germ line mutagenesis of the murine t region including a lethal allele at the quaking locus. *Proc. Natl. Acad. Sci. USA* **85**, 180–184. doi:10.1073/pnas.85.1.180
- Sparrow, D. B., McInerney-Leo, A., Gucevic, Z. S., Gardiner, B., Marshall, M., Leo, P. J., Chapman, D. L., Tasic, V., Shishko, A., Brown, M. A. et al. (2013). Autosomal dominant spondylocostal dysostosis is caused by mutation in TBX6. *Hum. Mol. Genet.* **22**, 1625–1631. doi:10.1093/hmg/ddt012
- Stott, D., Kispert, A. and Herrmann, B. G. (1993). Rescue of the tail defect of Brachyury mice. *Genes Dev.* **7**, 197–203. doi:10.1101/gad.7.2.197

- Takada, S., Stark, K. L., Shea, M. J., Vassileva, G., McMahon, J. A. and McMahon, A. P.** (1994). Wnt-3a regulates somite and tailbud formation in the mouse embryo. *Genes Dev.* **8**, 174-189. doi:10.1101/gad.8.2.174
- Watabe-Rudolph, M., Schlautmann, N., Papaioannou, V. E. and Gossler, A.** (2002). The mouse rib-vertebrae mutation is a hypomorphic Tbx6 allele. *Mech. Dev.* **119**, 251-256. doi:10.1016/S0925-4773(02)00394-5
- Wehn, A. K. and Chapman, D. L.** (2010). Tbx18 and Tbx15 null-like phenotypes in mouse embryos expressing Tbx6 in somitic and lateral plate mesoderm. *Dev. Biol.* **347**, 404-413. doi:10.1016/j.ydbio.2010.09.001
- White, P. H. and Chapman, D. L.** (2005). Dll1 is a downstream target of Tbx6 in the paraxial mesoderm. *Genesis* **42**, 193-202. doi:10.1002/gene.20140
- White, P. H., Farkas, D. R., McFadden, E. E. and Chapman, D. L.** (2003). Defective somite patterning in mouse embryos with reduced levels of Tbx6. *Development* **130**, 1681-1690. doi:10.1242/dev.00367
- White, P. H., Farkas, D. R. and Chapman, D. L.** (2005). Regulation of Tbx6 expression by Notch signaling. *Genesis* **42**, 61-70. doi:10.1002/gene.20124
- Wilkinson, D. G.** (1992). Whole mount in situ hybridization of vertebrate embryos. In *In Situ Hybridization: A Practical Approach* (ed. D. G. Wilkinson), pp. 75-83. Oxford: IRL Press.
- Wilkinson, D. G., Bhatt, S. and Herrmann, B. G.** (1990). Expression pattern of the mouse T gene and its role in mesoderm formation. *Nature* **343**, 657-659. doi:10.1038/343657a0
- Yasuhiko, Y., Haraguchi, S., Kitajima, S., Takahashi, Y., Kanno, J. and Saga, Y.** (2006). Tbx6-mediated Notch signaling controls somite-specific Mesp2 expression. *Proc. Natl. Acad. Sci. USA* **103**, 3651-3656. doi:10.1073/pnas.0508238103
- Yasuhiko, Y., Kitajima, S., Takahashi, Y., Oginuma, M., Kagiwada, H., Kanno, J. and Saga, Y.** (2008). Functional importance of evolutionarily conserved Tbx6 binding sites in the presomitic mesoderm-specific enhancer of Mesp2. *Development* **135**, 3511-3519. doi:10.1242/dev.027144